Bundling of double wall carbon nanotubes and Raman G band

P. Puech[*], S. Nanot[**], B. Raquet[**], J.M. Broto[**], M. Millot[**], A.W. Anwar[*], E. Flahaut[***] and W.S. Bacsa[*]

[*]CEMES, UPS, CNRS, Université de Toulouse
23 rue Jeanne Marvig, Toulouse 31055, France, wolfgang.bacsa@cemes.fr
[**]LNCMI, UPS, INSA, CNRS, Université de Toulouse
143 av. de Rangeuil, 31077 Toulouse, France
[***]CIRIMAT, UPS, CNRS, Université de Toulouse
118 route de Narbonne, 31062 Toulouse, France

ABSTRACT

We find that the Raman G band for individual double wall carbon nanotubes is split when the two walls are closely spaced or strongly coupled. We show that agglomeration of tubes into bundles leads to line broadening and overlapping of the G bands from the inner and outer tubes. This demonstrates that the observed broadening is not due to defects in the tube walls. We identify the tube helicity of an individual double wall tube. The consequence of our finding is that mapping of the Raman G band allows us to access the dispersion state of carbon nanotubes in a composite matrix.

Keywords: nanotubes, Raman spectroscopy, composites, dispersion

1 INTRODUCTION

The dispersion of carbon nanotubes in a polymer composite is a key challenge. The control of the dispersion state of carbon nanotubes (CNTs) allows reducing the percolation threshold. The formation of the percolation network in composites is used to evacuate electrical charges or for reinforcement. The percolation thresholds in CNT composites varies by more than two orders of magnitude (0.01-1w%) depending on tube type used [1]. The composition of carbon nanotube samples itself varies on a number of process parameters which are often not well controlled. As a result the agglomeration state and exact composition differs considerably. When mixing the tubes in the composite several additional process parameters play an important role in the final dispersion state of the tubes. To take advantage of the one dimensional nature of carbon nanotubes, it is essential to control their dispersion state to guarantee low percolation threshold. In double wall carbon nanotubes (DWs), the two walls are subject to a different environment. While the inner tube is surrounded by the outer tube, the outer tube is surrounded by the matrix or neighbouring DWs. As a result the interaction of the tube walls differs for the inner and outer tube which results in different spectroscopic positions of the Raman G band for inner and outer tubes.

DWs can be grown either by conversion of peadpods [2] or through the catalytic chemical vapor deposition method (CCVD) [3]. The wall spacing is typically smaller for CCVD [4] grown DWs while DWs grown from peapods show larger inter wall spacing [5]. This difference can be explained by the different growth conditions of the DWs. In the case of DWs grown with the CCV method, the inner and outer tubes are formed at the same time while in the case of peapod conversion, the inner tube is formed in the presence of a already present outer tube. Raman spectra of RBMs are consistent with this difference [4, 5]. The G band line shape also shows clear differences for the two types of DWs due to changes in the tube coupling. The pressure transmission on the inner tube is delaying for DWs grown from peapods as compard for DWs grown with the CCVD method [6]. The two types of DWs show also differences in the G'2D band. The G'2D band for DWs grown form peapods has two separated contributions due to inner and outer tubes while the G'2D band for DWs grown with the CCVD method shows one band with a shoulder similar to what is observed for graphite. We are here using DWs grown with CCVD and with small wall spacing.

To establish the difference in the Raman G band between individual and bundled DWs we have performed measurements on individual DWs and on isolated bundles of DWs on silicon oxide and compared the spectroscopic band positions and line broadening as a function of excitation wavelength.

2 EXPERIMENTAL

Raman spectra were acquired with a T64000 spectrometer from Horiba Jobin-Yvon. The laser power was measured after the objective. Polarization has been selected along the tube axis according to the scanning force microscopy images of the tube. We find that laser heating is less important for individual DWs in contact with the substrate or connected to the metal electrode. We use 1 mW with an objective of magnitude 100. We find that bundles of DWs are more sensitive to laser power. To reduce heating effects

on DW bundles we use a low laser power, typically 0.1 mW and an objective of magnitude 40 is used to increase the focal spot size (2 μm) decreasing the power density. All spectra have been recorded by integrating the signal from the scattered light for 100-500 seconds. We were able to increase the laser power up to 3 mW before the sample deteriorated.

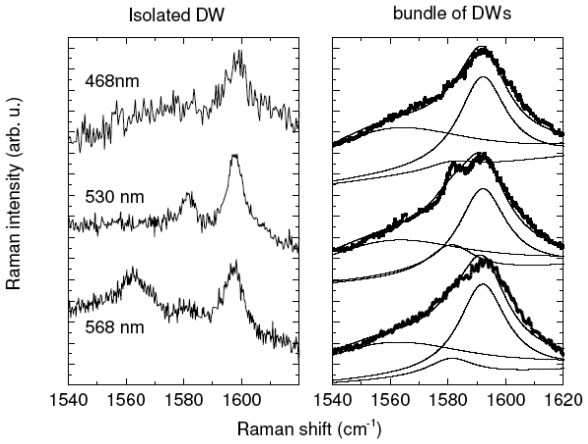

FIG 1: G band of individual DW (left side) and bundles of DWs (right side) using three excitation energies.

Fig. 1 shows the Raman G band region of the individual DW and bundled DWs excited with three different excitation wavelengths. By changing the excitation wavelength we find the resonance which is specific to the tube structure and this allows us to assign the tube structure of the inner and outer tube. The spectra from the isolated DW are narrower and contain up to three spectral bands. Bundles of DWs show a larger and asymmetric G band. The spectra of the DW bundles have been fitted by three Lorentzian line shapes using fixed spectral position and taking the relative intensities as a free parameter [6]. The half width at have maxima (HWHM) is considerable smaller for individual DWs. The G band of the inner and outer tube is 4±1 cm−1 which is the same HWHM observed for isolated SWs or for single layer graphene [17]. The HWHM in general depend on the number of defects and it has been shown that for SWs that the HWHM varies with applied voltage with a minimum value of 4 cm^{-1} [18, 19]. For bundles of DWs the HWHM is 10 cm^{-1}. The larger HWHM for bundles can be explained by the interaction with neighbouring tubes leading to heterogeneous line broadening. For comparison, pyrolytic graphite has a similar HWHM (7 cm^{-1}) [20].

For the individual DW, the spectral position of the G band of the inner tube is at 1580±2 cm^{-1} and for the outer tube at 1597±2 cm^{-1}. The spectral position of the inner tube is consistent with the extrapolated spectral position deduced from high pressure experiments [21] and when studying the influence by chemical doping of DWs [15]. The spectral position of the G band for the outer tube is high compared to the G band in single wall tubes. When changing the excitation energy, we can see considerable changes in the intensity of the inner tube reflecting changes in the resonance condition. At 568 nm an additional band is observed at 1563 cm^{-1} which has been previously observed and identified as being associated with electronic coupling with the environment and the outer tube [6].

To identify the tube structure of the inner and outer tube we use the electronic transition energies from the Kataura plot as reported by Araujo et al [13]. We can then estimate the transition energies for E^{S}_{11}, E^{S}_{22} and E^{M}_{11} where *S* denotes semiconducting tubes and *M* metallic tubes. For the E^{S}_{33} and E^{S}_{44} or E^{S}_{55} and E^{S}_{66}, we use for $\gamma_p = 0.305$ for unbound excitonic states as suggested by the authors where γ_p is a correction associated to exciton localisation. For the E^{M}_{22} transition, we use $\gamma_p = 0.305$ which fits well with the experimental results of Sfeir et al [22] reducing the error to less than 0.1 eV for the corresponding transition energies.

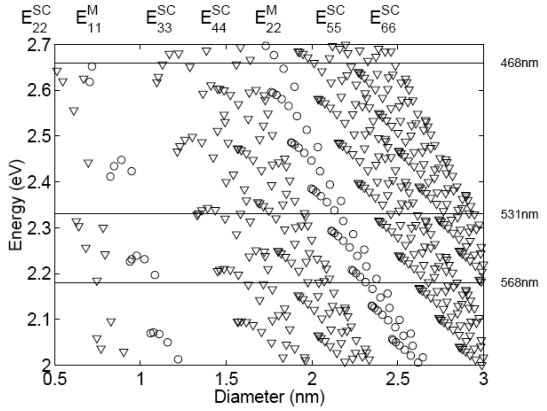

FIG. 2: Optical transition energies from Araujo et al [12] indicating the 3 different excitation wavelengths. The circles show the transition energies for metallic and the triangles show the transition energies for semiconducting tubes.

From the diameter histogram of our DW sample as determined by TEM, we consider 3 configurations with increasing diameter: M@S, S@M and S@S. We use the following notation for the four combinations of tubes for DWs: M@M, S@M, M@S, S@S (inner@outer). From height estimations using scanning force microscopy, we conclude that the M@S configuration with an outer diameter of 1.7 nm and an inner one of 1 nm is the most likely configuration for the DW investigated here. A S@S configuration would imply an outer diameter of 2.7 nm and an inner diameter of 2 nm. This configuration can be excluded by our preliminary electronic transport measurements which show a small on/off ratio in the

source-drain current vs. gate voltage dependence characteristic for metallic tubes [23]. From the gate voltage at the largest variation of the source drain current we find that the semiconducting tube is p doped.

We note that for a similar DW, M@S configuration and similar diameter, Villalpando-Paez et al [14] found a G band frequency of 1591 cm^{-1} without separating between contributions from the inner and the outer tube although the tube diameters are similar even so the samples have been grown using the CCVD method. Interestingly no splitting is observed here for the G'2D band while Villalpando-Paez et al [14] observe a clear splitting of the G'2D as in the case for DWs grown from the peapod method. This shows that the two tubes of DWs grown with the CCVD method can be either strongly coupled or can be decoupled as in the case for DWS grown with the peapod method. It is clear that the parameters used in the CCVD method play an important role in the inter wall spacing. In our case, the inner and outer tubes are strongly coupled, leading to a clear difference in the spectral positions. The G band position associated with the outer tube of the individual DW is high. We attribute this to charge transfer due to the proximity of the palladium contact.

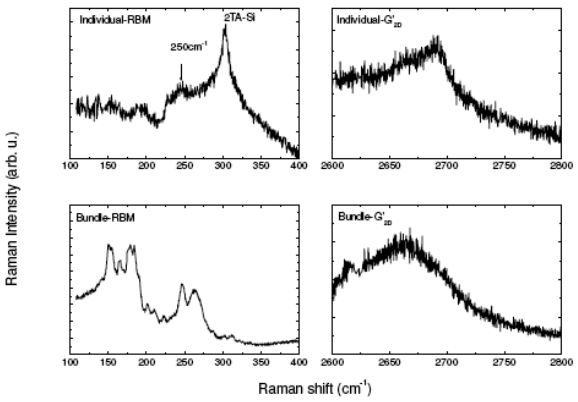

FIG 3: Frequency range of RBM and G'2D band of individual DW on SiO2 (Top) and DW bundles (below).

Fig. 3 shows the radial breathing mode (RBM) region and the second order D band (G'2D band) of the individual DW and bundled DWs using 531 nm excitation. The absence of sharp RBM bands in the case of individual tube indicates that the excitation does not coincide with the resonance maximum with neither of the two tubes. For bundles we observe several RBMs in the 140-180 cm^{-1} and 240-270 cm^{-1} spectral range. For the individual DW we observe a RBM band at 250 cm^{-1} consistent with an inner tube of 0.94 nm diameter and a less intense spectral band at 150 cm^{-1} consistent with the RBM of the outer tube (diameter: 1.61 nm). We use the constants for the determination of the diameter from the RBM frequency as reported by Telg et al [7]. The G'2D band for isolated tubes is less broad then those for bundles.

By varying the laser power from 1 mW to 3 mW for the individual DW on SiO_2 using 568 nm excitation, we observe changes in the G band of the outer tube and the disappearance of the additional spectral band at 1560 cm^{-1}. It has been previously found that this additional band is correlated with the shift of the G band of the outer tube with chemical doping [6]. The G band of the outer tube shifts to higher frequency and broadens with laser power while the G band of the inner tube remains at the same spectral position. A temperature increase, however, is known to shift the G band to lower frequency and broadening the band uniformly. The up shift and non-uniform broadening can be associated to stronger interaction with the substrate leading to a larger doping. Doping can lead to an up shift of the G band and can increase the HWHM for semi-conducting tubes [24]. This is compatible with a inner metallic and outer semiconducting tube.

3 DISCUSSION AND CONCLUSION

Electrical conductance measurements have shown that the signal associated to the outer tube can up shift or down shift and shows hysteresis when scanning the applied voltage [16]. As the tube lies on an insulating SiO_2 layer, the Fermi level of the outer tube can be influenced when illuminated through its interaction with its environment. By increasing the laser power at 568 nm close to the resonance for the E_{33} transition energy one increases the population of delocalised excitons on the outer tube. The presence of the substrate and the increased population of excitons in the outer tube modifies the electronic band structure. The outer tube is in contact with the substrate and the palladium contact. This is correlated with the disappearance with the additional band observed at 1560 cm^{-1}. The G band of the inner tube is not influenced by the laser power increase and shows that the inner tube can be used as a reference.

We find that coupled individual DWs show narrow and separated G bands corresponding to the inner and outer tube. The line-widths of the G band of the inner and outer tubes are comparable to what has been reported for individual SWs and single layer graphene. Bundling broadens the G band considerably. Using height estimation from scanning force microscopy, excitation wavelength and preliminary transport measurements, we can identify the tube configuration to be M@S. An increase of the laser power at 568nm leads to a preferential modification of the outer tube which is correlated with the disappearance of the additional band at 1560 cm^{-1} associated with the outer tube. Double wall carbon nanotubes with closely spaced walls are thus suitable to determine the dispersion state in a carbon nanotube polymer composite. Splitting of the Raman G band can be used as an indication of the presence of individual tubes as compared to broader G bands indicating the presence of bundled tubes.

REFERENCES

[1] W. Bauhofer et al Composite Science and Technology 69 (2009) 1486

[2] S. Bandow, M. Takizawa, K. Hirahara, M. Yudasaka, and S. Iijima, Chem. Phys. Lett. 337, 48 (2001)

[3] E. Flahaut, R. Bacsa, A. Peigney and Ch. Laurent, Chemical Communication 12, 1442 (2003)

[4] R. R. Bacsa, A. Peigney, Ch. Laurent, P. Puech, and W. S. Bacsa, Phys. Rev. B 65, 161404 (2002)

[5] R. Pfeiffer, F. Simon, H. Kuzmany, and V. N. Popov, Phys. Rev. B 72, 161404 (2005)

[6] P. Puech, A. Ghandour, A. Sapelkin, C. Tinguely, E. Flahaut, D.J. Dunstan and W. Bacsa, Phys. Rev. B 78, 045413 (2008)

[7] A. M. Rao, E. Richter, S. Bandow, B. Chase, P. C. Eklund et al., Science 275, 187 (1997)

[8] H. Telg, J. Maultzsch, S. Reich, F. Hennrich, and C. Thomsen, Phys. Rev. Lett. 93, 177401 (2004)

[9] C. Fantini, A. Jorio, M. Souza, M. S. Strano et al., Phys. Rev. Lett. 93, 147406 (2004)

[10] I.C. Gerber, P. Puech, A. Gannouni, and W. Bacsa, Phys. Rev. B79, 075423 (2009)

[11] H. Kataura, Y. Kumazawa, Y. Maniwa, I Umezu, S. Suzuki, Y. Ohtsuka and Y. Achiba, Sythetic Metals 103, 2555 (1999)

[12] S.M. Bachilo, M.S. Strano, C. Kittrell, R.H. Hauge, R.E. Smalley, and R.B. Weisman, Science 298, 2361 (2002)

[13] P.T. Araujo, S.K. Doorn, S. Kilina, S. Tretiak, E. Einarsson, S. Maruyama, H. Chacham, M.A. Pimenta and A. Jorio, Phys. Rev. Lett. 98, 067401 (2007)

[14] F. Villalpando-Paez, H. Son, D. Nezich, Y.P. Hsieh, J. Kong, Y.A. Kim, D. Shimamoto, H. Muramatsu, T. Hayashi, M. Endo, M. Terrones, and M.S. Dresselhaus, Nanoletters 8, 3879 (2008)

[15] G. Chen, S. Bandow, E.R. Margine, C. Nisoli, A.N. Kolmogorov, V.H. Crespi, R. Gupta, G.U. Sumanasekera, S. Iijima,and P.C. Eklund, Phys. Rev. Lett. 90, 257403 (2003)

[16] S. Yuan, Q. Zhang, Y. You, Z.X. Shen, D. Shimamoto and M. Endo, Nano Lett.9, 383, (2009)

[17] A. Das, S. Pisana, B. Chakraborty, S. Piscanec, S.K. Saha, U.V. Waghmare, K.S. Novoselov, H.R. Krishnamurthy, A.K. Geim, A.C. Ferrari, and A.K. Sood, Nature Nanotechn. 3, 210 (2008)

[18] J.C. Tsang, M. Freitag, V. Perebeinos, J. Liu and Ph. Avouris, Nature Nanotechn. (2007)

[19] A. Jorio, C. Fantini, M.S.S. Dantas, M.A. Pimenta, A.G. Souza Filho, Ge. G. Samsonidze, V.W. Brar, G. Dresselhaus, M. S. Dresselhaus, A. K. Swan, M. S. Unlu, B. B. Goldberg, and R. Saito, Phys. Rev. B 66, 115411 (2002)

[20] M. Hanfland, H. Beister, and K. Syassen, Phys. Rev. B 39, 12598 (1989)

[21] P. Puech, H. Hubel, D. Dunstan, R.R. Bacsa, C. Laurent, W.S. Bacsa, Phys. Rev. Lett. 93, 095506 (2004)

[22] M.Y. Sfeir, T. Beetz, F. Wang, L. Huang, X.M. Henry Huang, M. Huang, J. Hone, S. O'Brien, J.A. Msewich, T.F. Heinz, L. Wu Y. Zhu, and L.E. Brus, Science 312, 554 (2006)

[23] S. Wang, X. L. Liang, Q. Chen, Z. Y. Zhang, and L.-M. Peng, J. Phys. Chem. B 109, 17361 (2005)

[24] A. Das and A.K. Sood, Phys. Rev. B 79, 235429 (2009)